RSC Advances

PAPER

View Article Online
View Journal | View Issue

Cite this: *RSC Adv.*, 2023, **13**, 4578

Linear π-conjugated polycyclic compounds consisting of four-, five-, and six-membered rings: benzo[1″,2″:3,4;4″,5″:3′,4′]bis(cyclobuta[1,2-*c*]thiophene)†‡

Tatsuru Kuroiwa, Daisuke Asai, Shingo Hashimoto and Kazukuni Tahara *

Received 8th January 2023
Accepted 27th January 2023

DOI: 10.1039/d3ra00144j

rsc.li/rsc-advances

Linear π-conjugated polycyclic compounds, **BBCT**s, containing linearly annulated 5-, 4-, 6-, 4-, and 5-membered rings were produced *via* copper-mediated double intramolecular coupling reactions. The absorption spectra and electrochemical results confirmed their moderate optical energy gaps and high HOMO energy levels, respectively. In a crystalline state, the **BBCT** molecules adopt a herringbone structure, while the methylated molecules form slipped one-dimensional columns. The local and global aromaticity of the new polycyclic compounds is discussed based on the experimental results and theoretical predictions. The present fundamental findings are useful for the further design and synthesis of novel π-conjugated polycyclic compounds containing four-membered rings with potential applications in electronic materials.

Introduction

Acene has attracted research interest for over a century, including investigations of its fundamental properties and aromaticity and its applications in organic electronic devices.[1,2] The incorporation of heteroatom(s) into acene alters its stability, electronic properties, and intermolecular interaction modes. The incorporation of nitrogen or sulfur atoms modulates the energy levels of the frontier orbitals and crystal packing structures of acene, and some of these compounds are n- or p-type organic semiconducting materials, respectively.[3–8] Another approach to tailoring the properties of acene is the incorporation of hydrocarbon rings of different sizes. The inclusion of a four-membered ring (4MR) is particularly interesting because of its planarity and inherent anti-aromatic character.[9] Vollhardt and co-workers reported linear [*n*]phenylenes in which the 4MR bridges every benzene ring, resulting in unique local aromaticity and electronic properties compared to acene with similar sizes.[10–12] Linear π-conjugated polycyclic compounds containing 4MRs have also been reported to show intriguing photophysical and electronic properties owing to the modulated local aromaticity and frontier orbital energies.[13–16] Moreover, the incorporation of both nitrogen atoms and 4MRs into acene strongly affects these properties, with some of these compounds exhibiting distinguished semiconducting and luminescence properties.[17–26]

The incorporation of both sulfur atoms and 4MRs into acene affects its aromaticity and electronic properties. We previously investigated the geometries, electronic properties, and aromaticity of benzo[3,4]cyclobuta[1,2-*c*]thiophene (***c*BCT**) and its extended homologues using density functional theory (DFT) calculations (Fig. 1).[27] While the synthesis of ***c*BCT** was reported previously,[25,28] its extended homologues have not been experimentally explored. Among the homologues, benzo[1″,2″:3,4;4′,5″:3′,4′]bis(cyclobuta[1,2-*c*]thiophene) (**BBCT**) was chosen as the first test molecule for experimental investigation for the

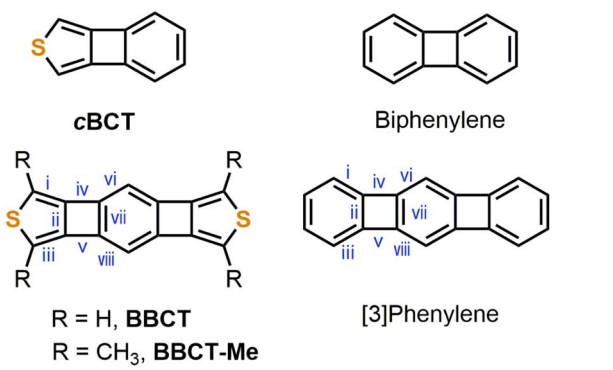

Fig. 1 Chemical structures of *c*BCT, biphenylene, BBCT, BBCT-Me, and [3]phenylene. Roman numerals on the BBCTs and [3]phenylene indicate bond positions.

Department of Applied Chemistry, School of Science and Technology, Meiji University, 1-1-1 Higashimita, Tama-ku, Kawasaki, Kanagawa, 214-8571, Japan. E-mail: tahara@meiji.ac.jp

† Dedicated to Professor Shigeru Yamago on the occasion of his 60th birthday.

‡ Electronic supplementary information (ESI) available. CCDC 2223524 and 2223525. For ESI and crystallographic data in CIF or other electronic format see DOI: https://doi.org/10.1039/d3ra00144j

following reasons. **BBCT** will be more stable than its b-type isomer.[27,29,30] The energy gap (E_{Gap}) and HOMO energy level of **BBCT** predicted by the DFT calculations are moderate due to the production of a p-type organic semiconducting material. **BBCT** will show moderate global aromaticity; the two fused 4MRs will attenuate the aromaticity of the central benzene ring and the fused thiophene ring at the 3,4-bond (c-type) with low electron density because its inherent diene character will attenuate the antiaromatic character of the 4MRs.[27,31–35] Finally, **BBCT** has a unique structural feature, *i.e.*, the linear annulation of 5-, 4-, 6-, 4-, and 5-membered rings.[36–43]

In this context, we herein report the synthesis, electronic properties, crystal structures, and aromaticity of **BBCT** and its methylated compound **BBCT-Me** and compare them with the properties and structure of [3]phenylene as a reference compound,[10] for future potential application of these molecules as p-type semiconducting materials.

Results and discussion

For the construction of the small, yet strained 4MRs, we chose a copper-mediated intramolecular coupling reaction of dibromobiaryls under ambient conditions.[12,44] We first tested the synthesis of biphenylene and ***c*BCT**. Biphenylene and ***c*BCT** were isolated in 54% and 29% yields from 2,2′-dibromobiphenyl and 3-bromo-4-(2-bromophenyl)thiophene (**2**), respectively (Scheme 1). The lower yield obtained for ***c*BCT** is attributed to the larger strain associated with 4MR formation between the rings of different sizes, as supported by DFT calculations (Fig. S1, ESI‡). While the isolated yield of ***c*BCT** is not high, it is higher than the reported values.[25,28,45] Thus, we employed this reaction for the synthesis of **BBCT**. Precursors **4a** and **4b** were synthesized *via* a palladium-catalyzed cross-coupling reaction between 3,4-dibromothiophenes and 1,4-dibromo-2,5-diiodobenzene. The double-fold 4MR formation in both **4a** and **4b** afforded **BBCT** and **BBCT-Me** in 4% and <1% (2% based on the NMR internal standard method) isolated yields, respectively. In the case of **BBCT-Me**, the addition of *N*,*N*,*N*′,*N*′-tetramethylethylenediamine (TMEDA) is needed due to the steric influence of the methyl groups. The **BBCT**s containing the strained 4MRs are stable under ambient conditions. As a reference compound, we synthesized [3]phenylene (see ESI‡).

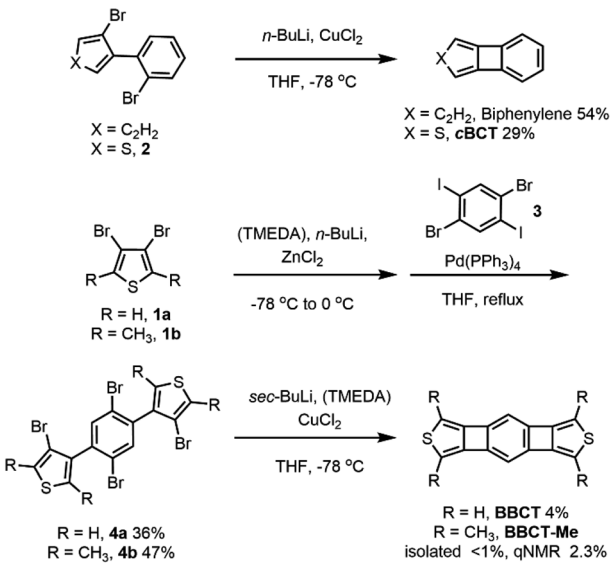

Scheme 1 Synthesis of biphenylene, *c*BCT, BBCT, and BBCT-Me.

Fig. 2 shows the absorption spectra of ***c*BCT**, **BBCT**, **BBCT-Me**, and [3]phenylene in CH_2Cl_2 at room temperature. The absorption spectrum of ***c*BCT** shows two strong bands with maxima at 348 and 249 nm. The absorption spectra of the **BBCT**s are similar, displaying strong bands with maxima at 423 and 285 nm for **BBCT** and 427 and 304 nm for **BBCT-Me**. The red shift in absorption for the **BBCT**s with respect to ***c*BCT** is due to the extension of π-electron conjugation. The absorption spectrum of [3]phenylene is similar to those of the **BBCT**s, although the very weak absorption band extends to 520 nm. The optical band gap ($E_{Opt.Gap}$) values estimated from the absorption edges are 3.43, 2.68, 2.69, and 2.38 eV for ***c*BCT**, **BBCT**, **BBCT-Me**, and [3]phenylene, respectively (Table 1). The smallest excitation energy (calc. $E_{excitation}$) values predicted by time-dependent (TD) DFT calculations at the B3LYP/6-311+G(d,p) level agree with the $E_{Opt.Gap}$ values. Moreover, TD-DFT calculations support that the lowest-energy transitions of these compounds involve the HOMO, LUMO, and LUMO+1 (Fig. S2, S3 and Tables 1, S2–S5, ESI‡). The blue shift of the adsorption edges of the **BBCT**s with respect to that of [3]phenylene is attributed to the lower LUMO level of [3]phenylene.

Cyclic voltammetry measurements of ***c*BCT**, **BBCT**, **BBCT-Me**, and [3]phenylene were conducted at room temperature in CH_2Cl_2 using $[n\text{-}Bu_4N][ClO_4]$ as the supporting electrolyte (Table 1 and Fig. 3). The cyclic voltammogram of ***c*BCT** shows one irreversible oxidation wave at E_{pa} = 1.23 V (Fc/Fc^+). Two irreversible oxidation waves were recorded in the voltammograms of **BBCT** and **BBCT-Me**, with the first oxidation waves peaking at E_{pa} = 0.59 and 0.38 V, respectively. [3]Phenylene also shows two irreversible oxidation waves, with the first peaking at E_{pa} = 0.47 V. The electrochemically derived HOMO energy levels (exp. E_{HOMO}) of ***c*BCT**, **BBCT**, and **BBCT-Me** were −5.7, −5.2, and −5.0 eV, respectively, based on the onsets of each first oxidation wave in the voltammograms (E_{onset}). These values qualitatively

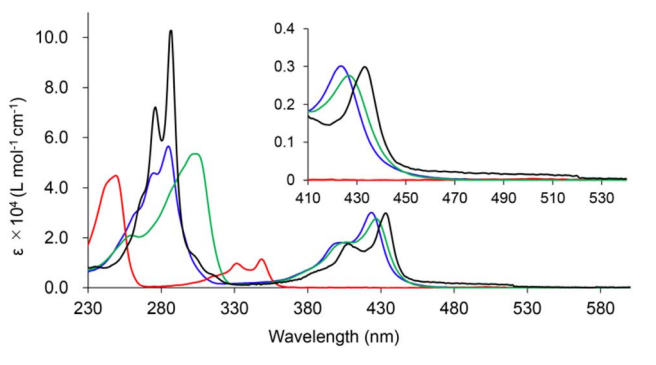

Fig. 2 UV-vis absorption spectra of *c*BCT (red), BBCT (blue), BBCT-Me (green) and [3]phenylene (black) at room temperature in CH_2Cl_2.

Table 1 Electronic properties of **BBCT**, **BBCT-Me**, ***c*BCT**, and [3]phenylene

Compound	λ_{edge} (nm)	Exp. $E_{Opt.Gap}$[a] (eV)	Calc. $E_{excitation}$[b] (eV)	Calc. E_{Gap}[c] (eV)	E_{onset} (V)	E_{pa} (V)	Exp. E_{HOMO}[d] (eV)	Calc. E_{HOMO}[c] (eV)
BBCT	463	2.68	2.78	3.47	0.39	0.59	−5.2	−5.35
BBCT-Me	461	2.69	2.87	3.53	0.21	0.38	−5.0	−5.09
***c*BCT**	362	3.43	3.72	4.51	0.86	1.23	−5.7	−5.83
[3]Phenylene	520	2.38	2.25	2.97	0.26	0.47	−5.1	−5.13

[a] Determined from the absorption edges in the UV-vis absorption spectra. [b] The smallest excitation energies estimated by TD-DFT calculations at the B3LYP/6-311+G(d,p) level of theory. [c] Estimated from the optimized geometries at the B3LYP/6-311+G(d,p) level of theory. [d] Derived from the onsets of the first oxidation waves in the cyclic voltammograms (Fig. 3).

agree with those predicted by DFT simulation (calc. E_{HOMO}, Table 1). These results suggest that the size of the π-conjugated system and methyl groups affect the electronic properties.[46] Based on comparison with the HOMO energy levels of thienoacenes with the same number of rings, the **BBCT**s are reasonable electron donors.[47,48]

Platelet single crystals of **BBCT** and **BBCT-Me** suitable for X-ray diffraction analysis were grown from THF/EtOH and CH_2Cl_2/hexane, respectively. Both compounds adopt virtually planar geometries, confirming the linearly annulated 5-, 4-, 6-, 4-, and 5-membered rings (Fig. 4a and 5a). The **BBCT** and **BBCT-Me** molecules pack in the $P2_1/c$ space group. The **BBCT** molecules adopt a herringbone structure (Fig. 4b and c).[49] Within the column consisting of molecules with the same orientation, the adjacent molecules slip completely with limited intermolecular contacts. The nearest interatomic distances between the carbon atoms in the same and different columns are 3.46 Å. The interatomic distances between the hydrogen and carbon atoms range from 2.73 to 3.26 Å, suggesting (C–H)–π interactions between the columns.[50] Moreover, there are close contacts between the sulfur and hydrogen atoms (3.09 Å).[51] On the other hand, the **BBCT-Me** molecules form slipped one-dimensional columns with two different orientations (Fig. 5b and c). The nearest interatomic distances of the carbon atoms of adjacent molecules within the column are 3.43 Å. The methyl groups of **BBCT-Me** are located on the thiophene rings of the adjacent molecules in the different columns with distances of 2.86 Å between the hydrogen atoms of the methyl groups and the centroid of the thiophene rings, indicating (C–H)–π interactions. The methyl groups of **BBCT-Me** are also close to the 4MRs of adjacent molecules within the column. The nearest distances between the hydrogen atoms of the methyl groups and the carbon atoms of the 4MRs are 2.78 Å, again indicating (C–H)–π interactions. The methyl groups influence the crystal packing structure of the **BBCT**s. The non-covalent interaction (NCI) plots[52] were calculated at the r^{2}SCAN-3c/def2-mTZVPP level of

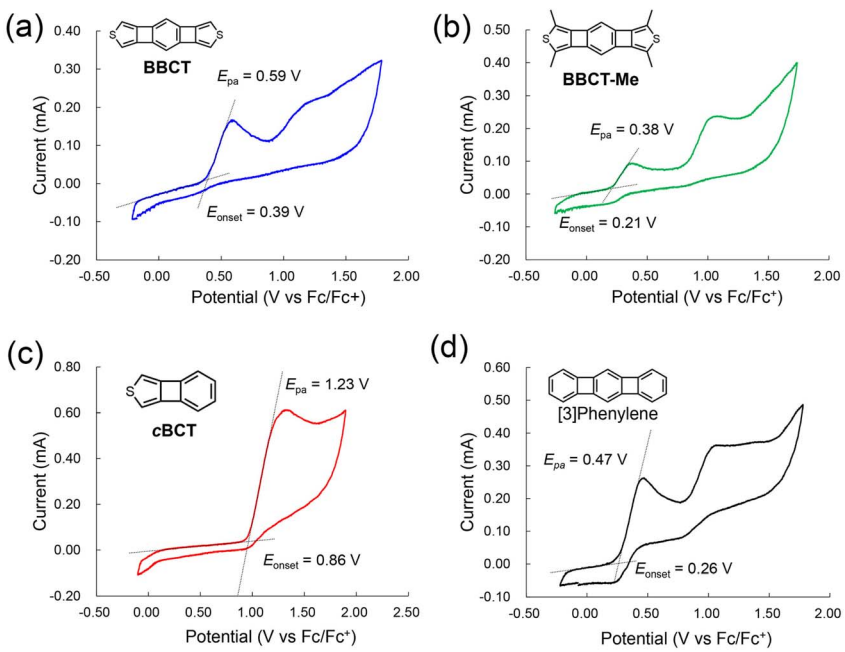

Fig. 3 Cyclic voltammograms of **BBCT** (a), **BBCT-Me** (b), ***c*BCT** (c), and [3]phenylene (d) in CH_2Cl_2 (concentration: 2 mM; supporting electrolyte: [*n*-Bu_4N][ClO_4]; scan rate: 100 mV s^{-1}). Black dotted lines are the linear extrapolations which were used for the estimation of the onset potentials (E_{onset}). The potentials are against the ferrocene/ferrocenium (Fc/Fc^+) couple. E_{pa}s are the peak top potentials of the first oxidation waves.

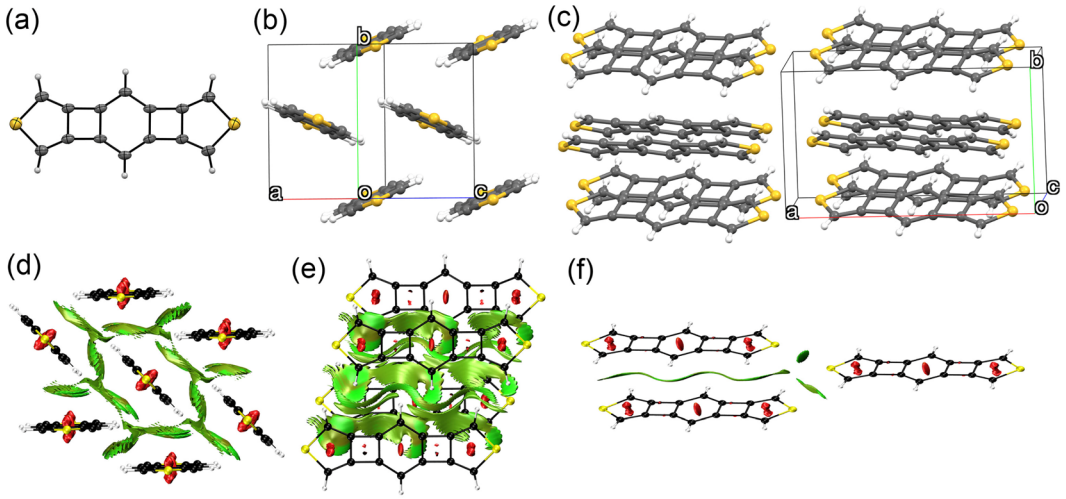

Fig. 4 Crystal structure of **BBCT**. (a) Molecular structure of **BBCT** with thermal ellipsoids at 30% probability. (b) Six molecules of **BBCT** viewed from the direction of the medium line of the unit cell vectors *a* and *c*. (c) Twelve molecules of **BBCT** viewed from the direction of the unit cell vector *c*. (d)–(f) NCI plots of the **BBCT** molecules in the crystal structure calculated at the r^{2}SCAN-3c/def2-mTZVPP level (isovalue: 0.60 a.u.). 2D reduced density gradient *vs.* sign(λ_2)ρ plots are shown in Fig. S10 (ESI‡).

theory[53] to visualize these interactions (Fig. 4d–f, 5d–f, S10 and S11‡). Charge-transfer integral calculations predict that the **BBCT** molecules show molecular orbital interactions in the herringbone structure (Fig. S12, ESI‡), implying potential in the application of p-type semiconducting material.

The local and global aromaticity of the novel polycyclic compounds is an intriguing subject. We analyzed the bond lengths of **BBCT**s from the crystal structures. The two shared and four non-shared bonds of the central benzene ring of the **BBCT**s are similar in length (Table 2 and Fig. S7, S8, ESI‡), indicating negligible bond length alternation. The shared bonds show single-bond character to reduce the electron density in the 4MRs.[27,35] As the structural criterion for the local aromaticity, we performed the harmonic oscillator model of aromaticity (HOMA).[54] The HOMA value of the central benzene ring of **BBCT** is large (0.88, Fig. S9, ESI‡), which is attributed to the small degree of bond length alteration rather than cyclic π-electron delocalization.[10] The thiophene rings retain diene character (Table 2). It should be noted that the lengths of the shared bonds in the 4MR differ by 0.018 Å between the benzene

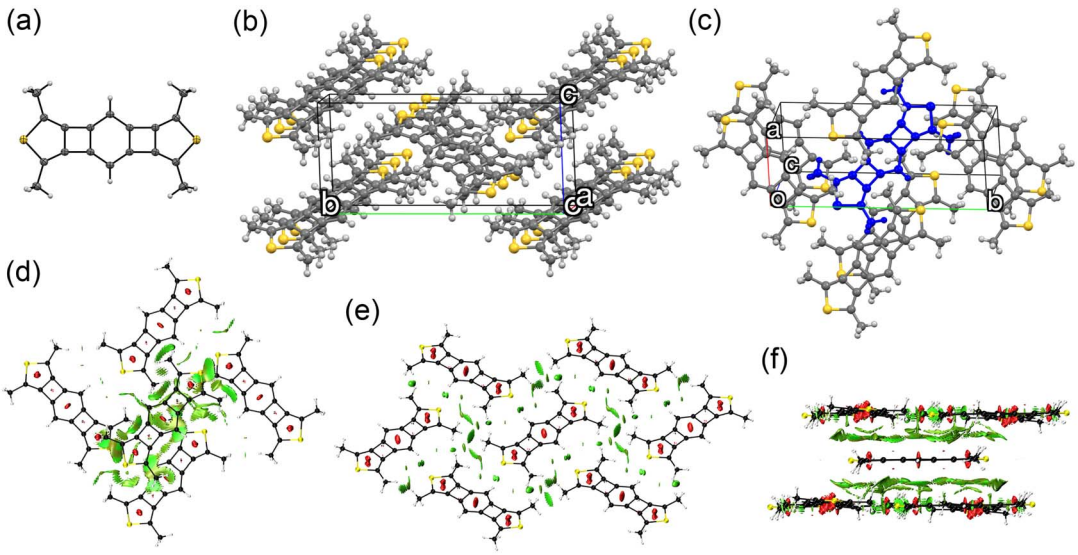

Fig. 5 Crystal structure of **BBCT-Me**. (a) Molecular structure of **BBCT-Me** with thermal ellipsoids at 30% probability. (b) Fifteen molecules of **BBCT-Me** viewed from the direction of the unit cell vector *a* showing slipped one-dimensional columns with two different orientations. (c) Eight molecules of **BBCT-Me** viewed from the unit cell vector *c*. The central molecule in which the methyl groups show short contacts with adjacent molecules is colored blue. (d)–(f) NCI plots of the **BBCT-Me** molecules in the crystal structure calculated at the r^{2}SCAN-3c/def2-mTZVPP level (isovalue: 0.60 a.u.). 2D reduced density gradient *vs.* sign(λ_2)ρ plots are shown in Fig. S11 (ESI‡).

Table 2 Bond lengths (Å) of **BBCT**, **BBCT-Me**, and [3]phenylene determined by X-ray single-crystal analysis

Compound[a]	i	ii	iii	iv	v	vi	vii	viii
BBCT	1.341(4)	1.443(3)	1.342(4)	1.505(3)	1.496(3)	1.384(3)	1.425(3)	1.387(3)
BBCT-Me	1.349(2)	1.443(2)	1.353(2)	1.502(2)	1.501(2)	1.393(2)	1.430(2)	1.389(2)
[3]Phenylene[b]	1.363(2)	1.419(2)	1.365(2)	1.514(2)	1.514(2)	1.392(2)	1.416(2)	1.390(2)

[a] Bond positions are described in Fig. 1. [b] Bond lengths of [3]phenylene were referred from ref. 55.

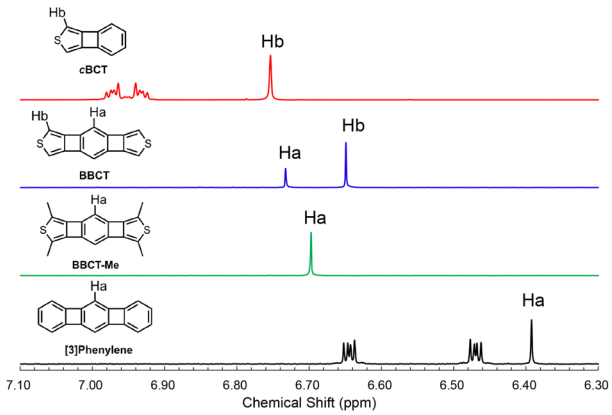

Fig. 6 ^{1}H NMR spectra of ***c*BCT** (red), **BBCT** (blue), **BBCT-Me** (green), and [3]phenylene (black) in acetone-d_6 at 25 °C.

and thiophene sides. Moreover, the shared bonds of the central benzene rings are elongated in **BBCT** compared with those of [3]phenylene,[55] indicating the larger strain of **BBCT**. This could be a factor in the low efficiency of 4MR construction in **BBCT**. As the measure of aromatic ring current effect, we compared the signals of the hydrogen atoms in the ^{1}H NMR spectra recorded in acetone-d_6 (Fig. 6). The signals of the hydrogen atoms (Ha) of **BBCT** and [3]phenylene resonated at 6.73 and 6.41 ppm, respectively, while those of the hydrogen atoms of the benzene ring in ***c*BCT** appeared at 7.02–6.90 ppm. The aromatic shielding effect from the diatropic ring currents of the central benzene ring is attenuated in **BBCT**, although it is still stronger than that in [3]phenylene. A similar trend was observed in the chemical shift of the hydrogen atoms attached to the thiophene ring (6.74 and 6.64 ppm for ***c*BCT** and **BBCT**, respectively). The nucleus-independent chemical shift (NICS) scans and calculated current paths and strengths also agree with the above observations (Fig. S4–S6, ESI‡).[27,56] The local aromaticity of the central benzene ring and thiophene rings is attenuated in **BBCT**. Moreover, theoretically predicted paratropic character of the 4MRs in **BBCT** is weaker than those of [3]phenylene, indicating the limited anti-aromatic character of the 4MRs in **BBCT**.[27] Overall, **BBCT** has moderate global aromaticity.

Conclusions

In conclusion, we synthesized a new family of linearly fused polycyclic compounds, **BBCT**s, containing the strained 4MRs that bridge thiophene and benzene rings. UV-vis absorption and electrochemical investigations confirmed that the **BBCT**s have moderate $E_{Opt.Gap}$ values and high HOMO energy levels. X-ray single-crystal analysis revealed that **BBCT** and **BBCT-Me** adopt herringbone and one-dimensional columnar structures, respectively. The structural features derived from the X-ray single crystal analysis and the aromatic ring current effect estimated by the ^{1}H NMR spectra indicated moderate aromatic character in **BBCT**. This finding is useful for producing novel organic materials based on polycyclic compounds containing 4MRs that bridge thiophene and benzene rings.

Author contributions

Conceptualization: KT. Investigation, experimental design, and formal analysis: TK, DA, SH. Experimental data collection: TK, DA, SH. Validation: TK, DA, SH. Project administration: KT. Funding acquisition: KT. Resources: KT. Writing (original draft): TK, KT. Writing (review & editing): TK, SH, KT.

Conflicts of interest

There are no conflicts to declare.

Acknowledgements

This work was supported by the Tokuyama Science Foundation. We thank Prof. Noriharu Nagao (Meiji University) for his support with the single-crystal X-ray diffraction analyses.

References

1 J. E. Anthony, *Angew. Chem., Int. Ed.*, 2008, **47**, 452–483.
2 M. Randić, *Chem. Rev.*, 2003, **103**, 3449–3605.
3 U. H. F. Bunz, *Acc. Chem. Res.*, 2015, **48**, 1676–1686.
4 B. Djukic and D. F. Perepichka, *Chem. Commun.*, 2011, **47**, 12619–12621.
5 X. Shi, T. Y. Gopalakrishna, Q. Wang and C. Chi, *Chem.–Eur. J.*, 2017, **23**, 8525–8531.
6 T. Yamamoto and K. Takimiya, *J. Am. Chem. Soc.*, 2007, **129**, 2224–2225.
7 M. Mamada and Y. Yamashita, in *Polycyclic Arenes and Heteroarene*, ed. Q. Miao, Wiley-VCH Verlag GmbH & Co. KGaA, Weinheim, Germany, 2016, pp. 277–308.
8 M. L. Tang, T. Okamoto and Z. Bao, *J. Am. Chem. Soc.*, 2006, **128**, 16002–16003.
9 W. C. Lothrop, *J. Am. Chem. Soc.*, 1941, **63**, 1187–1191.
10 B. C. Berris, G. H. Hovakeemian, T.-H. Lai, H. Mestdagh and K. P. C. Vollhardt, *J. Am. Chem. Soc.*, 1985, **107**, 5670–5687.

11 C. Dosche, H.-G. Löhmannsröben, A. Bieser, P. I. Dosa, S. Han, M. Iwamoto, A. Schleifenbaum and K. P. C. Vollhardt, *Phys. Chem. Chem. Phys.*, 2002, **4**, 2156–2161.
12 M. Watanabe and T. Ohashi, *Jpn. Kokai Tokkyo Koho*, 2008, JP2008247853A.
13 R. R. Parkhurst and T. M. Swager, *J. Am. Chem. Soc.*, 2012, **134**, 15351–15356.
14 Z. Jin, Y. C. Teo, S. J. Teat and Y. Xia, *J. Am. Chem. Soc.*, 2017, **139**, 15933–15939.
15 Z. Jin, Z.-F. Yao, K. P. Barker, J. Pei and Y. Xia, *Angew. Chem., Int. Ed.*, 2019, **58**, 2034–2039.
16 J. Wang, M. Chu, J.-X. Fan, T.-K. Lau, A.-M. Ren, X. Lu and Q. Miao, *J. Am. Chem. Soc.*, 2019, **141**, 3589–3596.
17 J. M. Blatchly, J. F. W. McOmie and S. D. Thatte, *J. Chem. Soc.*, 1962, 5090–5095.
18 M. P. Cava, D. R. Napier and R. J. Pohl, *J. Am. Chem. Soc.*, 1963, **85**, 2076–2080.
19 S. Hünig and H. Pütter, *Chem. Ber.*, 1977, **110**, 2532–2544.
20 S. Yang, D. Liu, X. Xu and Q. Miao, *Chem. Commun.*, 2015, **51**, 4275–4278.
21 S. Yang, M. Chu and Q. Miao, *J. Mater. Chem. C*, 2018, **6**, 3651–3657.
22 S. Yang, B. Shan, X. Xu and Q. Miao, *Chem.–Eur. J.*, 2016, **22**, 6637–6642.
23 P. Biegger, M. Schaffroth, C. Patze, O. Tverskoy, F. Rominger and U. H. F. Bunz, *Chem.–Eur. J.*, 2015, **21**, 7048–7052.
24 P. Biegger, M. Schaffroth, O. Tverskoy, F. Rominger and U. H. F. Bunz, *Chem.–Eur. J.*, 2016, **22**, 15896–15901.
25 V. Engelhardt, J. G. Garcia, A. A. Hubaud, K. A. Lyssenko, S. Spyroudis, T. V. Thimofeeva, P. Tongwa and K. P. C. Vollhadt, *Synlett*, 2011, 280–284.
26 Y. C. Teo, Z. Jin and Y. Xia, *Org. Lett.*, 2018, **20**, 3300–3304.
27 S. Hashimoto and K. Tahara, *J. Org. Chem.*, 2019, **84**, 9850–9858.
28 P. J. Garratt and K. P. C. Vollhardt, *J. Chem. Soc. D*, 1970, 109.
29 J. W. Barton and D. J. Lapham, *Tetrahedron Lett.*, 1979, **20**, 3571–3572.
30 J. Nakayama, *J. Synth. Org. Chem., Jpn.*, 1994, **52**, 308–317.
31 F. Fringuelli, G. Marino, A. Taticchi and G. A. Grandolini, *J. Chem. Soc., Perkin Trans.*, 1974, **2**, 332–337.
32 C. K. Frederickson, L. N. Zakharov and M. M. Haley, *J. Am. Chem. Soc.*, 2016, **138**, 16827–16838.
33 Y. Ohtomo, K. Ishiwata, S. Hashimoto, T. Kuroiwa and K. Tahara, *J. Org. Chem.*, 2021, **86**, 13198–13211.
34 S. Hashimoto, R. Kishi and K. Tahara, *New J. Chem.*, 2022, **46**, 22703–22714.
35 S. Hashimoto and K. Tahara, *Chemistry*, 2022, **4**, 1546–1560.
36 D. Cagardová, M. Michakík, P. Poliak and V. Lukeš, *J. Mol. Struct.*, 2019, **1175**, 297–306.
37 D. N. Nicolaides, *Synthesis*, 1977, 127–129.
38 M. L. Leow and J. A. H. MacBride, *Tetrahedron Lett.*, 1984, **25**, 4283–4284.
39 A. Fukazawa, H. Oshima, Y. Shiota, S. Takahashi, K. Yoshizawa and S. Yamaguchi, *J. Am. Chem. Soc.*, 2013, **135**, 1731–1734.
40 A. Fukazawa, H. Oshima, S. Shimizu, N. Kobayashi and S. Yamaguchi, *J. Am. Chem. Soc.*, 2014, **136**, 8738–8745.
41 P. J. Mayer, O. E. Bakouri, T. Holczbauer, G. F. Samu, C. Janáky, H. Ottosson and G. London, *J. Org. Chem.*, 2020, **85**, 5158–5172.
42 T. Gazdag, P. J. Mayer, P. P. Kalapos, T. Holczbauer, O. E. Bakouri and G. London, *ACS Omega*, 2022, **7**, 8336–8349.
43 M. Nishijima, K. Mutoh, R. Shimada, A. Sakamoto and J. Abe, *J. Am. Chem. Soc.*, 2022, **144**, 17186–17197.
44 S. M. H. Kabir, M. Hasegawa, Y. Kuwatani, M. Yoshida, H. Matsuyama and M. Iyoda, *J. Chem. Soc., Perkin Trans.*, 2001, 159–165.
45 P. J. Garratt and K. P. C. Vollhardt, *J. Am. Chem. Soc.*, 1972, **94**, 7087–7092.
46 M. Bendikov, F. Wudl and D. F. Perepichka, *Chem. Rev.*, 2004, **104**, 4891–4945.
47 S. Shinamura, I. Osaka, E. Miyazaki, A. Nakao, M. Yamagishi, J. Takeya and K. Takimiya, *J. Am. Chem. Soc.*, 2011, **133**, 5024–5035.
48 M. L. Tang, A. D. Reichardt, T. Siegrist, S. C. B. Mannsfeld and Z. Bao, *Chem. Mater.*, 2008, **20**, 4669–4676.
49 M. D. Curtis, J. Cao and J. W. Kampf, *J. Am. Chem. Soc.*, 2004, **126**, 4318–4328.
50 M. Nishio, M. Hirota and Y. Umezawa, *The CH/π Interaction: Evidence, Nature, and Consequences*, Wiley-VCH, New York, 1998.
51 H. A. Fargher, T. J. Sherbow, M. M. Haley, D. W. Johnson and M. D. Pluth, *Chem. Soc. Rev.*, 2022, **51**, 1454–1469.
52 E. R. Johnson, S. Keinan, P. Mori-Sánchez, J. Contreras-García, A. J. Cohen and W. Yang, *J. Am. Chem. Soc.*, 2010, **132**, 6498–6506.
53 S. Grimme, A. Hansen, S. Ehlert and J.-M. Mewes, *J. Chem. Phys.*, 2021, **154**, 064103.
54 J. Kruszewski and T. M. Krygowski, *Tetrahedron Lett.*, 1972, **13**, 3839–3842.
55 A. Schleifenbaum, N. Feeder and K. P. C. Vollhardt, *Tetrahedron Lett.*, 2001, **42**, 7329–7332.
56 P. v. R. Schleyer, C. Maerker, A. Dransfeld, H. Jiao and N. J. R. van Eikema Hommes, *J. Am. Chem. Soc.*, 1996, **118**, 6317–6318.